OFFICE OF NAVAL RESEARCH

Contract N00014-91-J-1927

R&T Code 413v001

Technical Report No. 10



# ELECTRIC FIELD INDUCED PHENOMENA IN STM: TIP DEFORMATION AND AU(111)-SURFACE PHASE TRANSITIONS DURING TUNNELING SPECTROSCOPY EXPERIMENTS

by

JOACHIM HOSSICK SCHOTT AND HENRY S. WHITE

Prepared for Publication in

Physical Review B

University of Minnesota
Department of Chemical Engineering and Materials Science
Minneapolis, MN 55455

March 20, 1993





# REPORT DOCUMENTATION PAGE

Form Approved
OMB No. 0704-0188



| 1. AGENCY USE ONLY (Leave blank) | 2. REPORT DATE | 3. REPORT TYPE AND DATES COVERED |
|---|---|---|
| | March 20, 1993 | Technical 6/30/92 - 3/31/93 |

**4. TITLE AND SUBTITLE**
ELECTRIC FIELD INDUCED PHENOMENA IN STM: TIP DEFORMATION AND AU(111)-SURFACE PHASE TRANSITIONS DURING TUNNELING SPECTROSCOPY EXPERIMENTS

**5. FUNDING NUMBERS**
N00014-91-J-1927

**6. AUTHOR(S)**
JOACHIM HOSSICK SCHOTT AND HENRY S. WHITE

**7. PERFORMING ORGANIZATION NAME(S) AND ADDRESS(ES)**
Dept. of Chemical Engineering and Materials Science
University of Minnesota

**8. PERFORMING ORGANIZATION REPORT NUMBER**
Technical Report No. 10

**9. SPONSORING/MONITORING AGENCY NAME(S) AND ADDRESS(ES)**
Office of Naval Research
800 North Quincy Street
Arlington, VA 22217

**10. SPONSORING/MONITORING AGENCY REPORT NUMBER**

**11. SUPPLEMENTARY NOTES**

**12a. DISTRIBUTION/AVAILABILITY STATEMENT**
Unclassified/Unlimited

**12b. DISTRIBUTION CODE**

**13. ABSTRACT** *(Maximum 200 words)*

We report electric field induced phase transitions of Au(1'1) surfaces and electric field stress induced elongations of Pt-Ir and Au tips during current voltage measurements with an STM in air. Transitions between the reconstructed $\sqrt{3}$ x 22 and the unreconstructed 1x1 phase of the Au(111) surface are attributed to changes in the electronic surface excess charge density induced by the electric field between tip and sample. Elongations of STM tips during tunneling spectroscopy give rise to a distinct non-linear current-voltage response at tip-to-sample biases greater than ~|0.5V|. Similar behaviour is observed during tunneling measurements on pyrolytic graphite and oxidized Ag surfaces. Extensive elongations can result in tip-sample point-contact and tip-fracture. Artificially low values of the apparent barrier height are shown to result from tip elongation.

| 14. SUBJECT TERMS | 15. NUMBER OF PAGES |
|---|---|
| | 32 |
| | 16. PRICE CODE |

| 17. SECURITY CLASSIFICATION OF REPORT | 18. SECURITY CLASSIFICATION OF THIS PAGE | 19. SECURITY CLASSIFICATION OF ABSTRACT | 20. LIMITATION OF ABSTRACT |
|---|---|---|---|
| Unclassified | UL | | |

# Electric Field Induced Phenomena in STM: Tip Deformations and Au(111)-Surface Phase Transitions during Tunneling Spectroscopy Experiments

Joachim Hossick Schott and Henry S. White
Department of Chemical Engineering & Materials Science
University of Minnesota
Minneapolis, MN 55455

## Abstract

We report electric field induced phase transitions of Au(111) surfaces and electric field stress induced elongations of Pt-Ir and Au tips during current voltage measurements with an STM in air. Transitions between the reconstructed $\sqrt{3}$ x 22 and the unreconstructed 1x1 phase of the Au(111) surface are attributed to changes in the electronic surface excess charge density induced by the electric field between tip and sample. Elongations of STM tips during tunneling spectroscopy give rise to a distinct non-linear current-voltage response at tip-to-sample biases greater than ~|0.5V|. Similar behaviour is observed during tunneling measurements on pyrolytic graphite and oxidized Ag surfaces. Extensive elongations can result in tip-sample point-contact and tip-fracture. Artificially low values of the apparent barrier height are shown to result from tip elongation.

submitted to *Phys. Rev. B*, July 1992

## Introduction

The measurement of the tunneling current, I, as a function of the applied bias voltage, $V_b$, between a spacially fixed tip and a sample using the scanning tunneling microscope (STM) has received a great deal of attention from various research groups in recent years. Analyses of I vs. $V_b$ curves (and/or their first and second derivatives), are used to characterize the electronic structure of the sample surface (e.g. the energetics and local densities of electronic surface and bulk states[1-7]), as well as to investigate fundamental aspects of tunneling phenomena (e.g., Coulomb blockade induced single electron tunneling[8,9])

The analysis of tunneling spectroscopy (TS) data obtained in STM experiments generally relies on the assumption that both the tip and the sample surface remain mechanically stable during the I-V measurement. However, we have shown in a preceding paper[10] that the electric field between a Pt(70%)Ir(30%)-tip and a Au(111) surface can lift and induce the $\sqrt{3}$ x 22 reconstruction of this surface at bias voltages commonly used in TS and STM experiments. Hence, since the atomic structure of the sample surface can change as a function of the applied bias, it seems reasonable to anticipate that the tip structure can change, too. This conclusion motivated the present study.

Very little has been reported concerning the effects of the electric field on the mechanical stability of tip and sample in STM[10-13]. Yet it is known from field-ion-microscopy studies that a field of ~1V/Å, which is easily realized in an STM, can result in mechanical stresses which can deform or even rupture the tip[14-16]. In this paper, we present a detailed investigation of I-V characteristics in tunneling spectroscopy experiments performed with Pt-Ir and Au tips on reconstructed Au(111), oxidized Ag and highly ordered pyrolytic graphite (HOPG) surfaces. Measurements are made in the bias voltage range $-3V \leq V_b \leq 3V$, i.e., well below the onset of field emission[1]. We show that field induced deformation of the STM tip during TS measurements has a significant effect on

the shape of the measured I-V characteristics. Artificially low barrier heights result from this instability.

## Experimental

Our experiments were performed in air with a Digital Instruments Nanoscope II(TM) scanning tunneling microscope[17], in which the tip is held at virtual ground and the bias voltage $V_b$ is applied to the sample. All images reported here were recorded in the constant current mode using a scan rate of 8.6 hz, and consist of 400 x 400 data points. Images were low pass filtered once.

TS experiments were performed by measuring the tunneling current I as a function of the ramped bias voltage V. The tip is placed in the center of a surface area which is imaged *before* and *after* each current voltage measurement. For all I-V data presented here, bias voltage ramping always starts at the positive limit of the selected voltage scan window. Typical scan times were ~0.5 sec. All I-V data are reported without filtering, smoothing or averaging. *Before* the actual I-V measurement, a tip-sample distance s is established by adjusting the feed back loop of the instrument with a programmable gap-resistance $R_{set} = V_{set}/I_{set}$. The feedback is then disabled and the tunneling current is measured as a function of the ramp voltage.

Effective tunneling barrier heights $\phi_{eff}$ were estimated from the measured dependence of the tunneling current on the gap separation. In this experiment, an arbitray initial tip-sample distance $s_0$ is established by adjusting the feedback loop with a gap resistance $R_{set}$. The feed back loop is then disabled and the gap spacing s is increased by applying an external voltage $V_z$ to the z-piezo. The current I is recorded as a function of the tip displacement $\Delta s = s - s_0$. The initial sample bias voltage $V_{set}$ ($=V_b$ in this experiment) remains constant during the I vs. $\Delta s$ measurement. Since the tunneling current I is proportional to $V_b \exp(-1.025 s \sqrt{\phi})$, a plot of ln(I) vs. $\Delta s$ has a slope of $\sim\sqrt{\phi_{eff}}$, or, $\phi_{eff} \sim (d\ln(I)/ds)^2$. [18]

$\sqrt{3}$ x 22 reconstructed Au(111) samples were prepared according to the procedure given by Hsu and Cowley[19]: one end of a ~2cm piece of Au wire was melted to form a sphere of 1-2mm diameter in a hydrogen/oxygen flame. Upon cooling in air or Argon, optically highly reflective facettes appear on the sphere which proof to be atomically flat in STM. Further annealing of a sphere in a cooler, hydrogen rich flame for about 2 min. typically results in a highly ordered $\sqrt{3}$ x 22 surface within the facet area. Oxidized Ag samples were prepared in a similar manner: one end of a 2 cm piece of Ag-wire ($\phi$ = 0.5mm, 99.995% purity, Aesar/Johnson Mathey) was melted in a hydrogen/oxygen flame to form a ball of 1-2 mm diameter upon solidification in air. Unlike gold, silver does not form atomically smooth crystalline facettes upon cooling. This is expected because silver oxidizes readily in air. HOPG surfaces were prepared by cleaving HOPG (Union Carbide, Grade B) immediately prior to STM and TS measurements. Tips were mechanically cut from Pt(70%)/Ir(30%) wire (0.1 mm diameter, Aesar/Johnson Mathey) and gold wire (99.999% purity, 50 μm diameter, Aesar/Johnson Mathey). Before cutting, the wires were heated to a white and red glow, respectively, in a hydrogen flame to remove organic surface contaminants.

## Results and Discussion

*Field induced surface changes on Au(111)*

The motivation for this TS study is based on our previously reported observation[10] that the $\sqrt{3}$ x 22 reconstruction of the Au(111) surface can be lifted and induced as a function of the bias voltage $V_b$ during STM imaging. The reconstructed Au(111) $\sqrt{3}$ x 22 surface is imaged in STM as parallel pairs of corragation lines (height ~ 0.2Å) running in the <112> direction with a pair-to-pair separation of ~63Å[20-22]. Long range features of this construction include domain structures separated by ~ 250Å and rotated $\pm 120^{o}$ with respect to each other, i.e. zig-zag patterns of parallel lines ("herringbone" pattern)[21]. The reconstruction can be rationalized with a tensile surface stress, arising from charge redistributions of mainly sp-electrons at the surface. This stress causes uniaxial compression of the topmost layer interatonic bond distances by about 5% in the <110> direction. In brief, the results from our previous work[10] can be summarized as follows: the $\sqrt{3}$ x 22 reconstruction features are stable and unaffected by continued STM imaging over a wide range of negative and low to moderate positive sample biases ($V_b \leq$ ~+0.5 V). Scanning with a positive sample bias $V_b$ of ~1.5V, however, completely lifts the reconstruction within the geometrical scan window. Negative biases $V_b \leq$-0.5V induce a transition from the 1x1 to the $\sqrt{3}$ x 22 reconstructed phase. We concluded that the sign and magnitude of the induced surface excess charge during the STM experiment determines the relative stability of the respective surface phases. Figs. 1 and 2 demonstrate, that these phase transitions can also be observed in combined STM/TS experiments when the bias during the I-V measurement is scanned to sufficiently positive or negative values. For example, Fig. 1a shows an STM image of a $\sqrt{3}$ x 22 reconstructed Au(111) surface area obtained with a moderate bias of -125 mV. Performing a I-V measurement (Fig. 1b) in the center of the imaged area leaves the surface unchanged when the sample bias during the I-V measurement is negative (e.g., 0 to -1V in Fig. 1b), as is evidenced by the image shown in Fig. 1c, which was taken immediately after the I-V measurement shown in Fig. 1b.

Voltage excursions to higher positive sample biases (e.g., 0 to +1V in Fig. 1d), however, partially lift the reconstruction in the area of the tip position. This can be observed in the image shown in Fig. 1e, taken immediately after the I-V scan shown in Fig. 1d. This latter image is noisier than the images shown in Fig. 1a and 1c. This is to be expected since the $\sqrt{3}$ x 22 $\rightarrow$ 1x1 transition requires transport of surface atoms in the transition area as demonstrated in the previous study[10].

Fig. 2 shows the inverse phenomenon measured on a different sample with a different tip. First, a small unreconstructed area was created on the $\sqrt{3}$ x 22 surface (Fig. 2a) by applying positive sample biases in an I-V experiment performed before taking the image. Two I-V measurements at large negative biases were then made over the same surface section (Figs. 2b and 2d). Images recorded following the I-V measurements show new reconstruction features in the previously unreconstructed area (Figs. 2c and 2e). In these experiments, bias voltage excursions smaller than ~ |0.5V| do not result in any significant surface changes. Tunneling spectroscopy measurements utilizing both negative and positive bias voltages clearly also effect the surface (Figs. 2f-2i). However, the effect appears to be merely a movement of reconstruction features rather than a phase transition.

Structural changes in the surface during the TS experiment must also effect the I-V response. For example, if a corrugation line on the $\sqrt{3}$ x 22 surface of height ~0.2Å moves under the apex of the tip, the corresponding change in the geometrical tunneling barrier will produce a change in the measured tunneling current. A comparison between the I-V curves in Fig. 1b and 1d shows that the curve obtained upon inducing the $\sqrt{3}$ x 22 --> 1 x 1 transition under the tip (Fig. 1d) is considerably noisier than the curve obtained upon ramping negative biases (Fig. 1b), which leaves the surface unchanged. We speculate that thé noise observed in the I-V curves shown in Fig. 2 may be due to lifting, creation or movement of reconstruction features under the tip.

*Electric field induced tip changes*

The shapes of the I-V curves shown in Fig. 1 and Fig. 2 (obtained with different Pt-Ir-tips) are markedly different and represent the two basic current voltage responses reported in the literature for Au(111)[23-25]. Whereas the curves in Fig. 2 are linear over the entire measured bias voltage window ($-3V \leq V_b \leq +3V$), those in Fig. 1 are linear only in a smaller voltage range around 0 V. A strong non-linear behaviour is observed in Fig. 1 at larger bias voltages, $V_b > \sim |0.5\ V|$. Based on experiments using ~100 different tips, we find that I-V measurements on reconstructed Au(111) exhibit non-linear curve shapes for 60% of the tips, at bias voltages exceeding |0.5 V|. (Only tip-sample systems yielding a reasonable image of the $\sqrt{3}$ x 22-Au(111) surface are included in the test set. Therefore, the mechanism suggested by Coombs and Pethica[26], in which a non-conductive particle may be trapped between tip and sample, yielding physically unreal images, can be ruled out for the experiments reported here.) The remaining 40% of the tips tested yield a linear I-V response in voltage scan windows as large as $-3V \leq V_b \leq +3V$. Since a linear I-V curve might be expected for a metal-vacuum-metal tunnel junction, it can be argued, that surface contaminants play a part in inducing the non-linear I-V behaviour observed here. However, all I-V measurements were performed exclusively on reconstructed Au(111) samples. Since the formation of the reconstruction requires a clean surface layer we can safely assume that we are dealing with clean gold. Clearly, we can not rule out the presence of a mobile and, therefore, undetected adsorbate layer. If this was of a measurable influence, however, a tip yielding a linear current voltage response at one surface location should yield a non-linear response at later times or at different locations. This was observed only in a few cases. One may further argue, that the tip surface might be contaminated or oxidized. This is most likely to be true for *all* Pt-Ir tips operated in air, since for both constituents of the alloy, it is difficult to obtain and maintain a clean surface, even in ultrahigh vacuum environments. If surface oxides on Pt-Ir tips induce

characteristic non-linear features in the current voltage response on Au(111), such features should always be found on oxidized surfaces. The linear I-V curve obtained on an oxidized Ag surface with a Pt-Ir tip shown in Fig. 3a demonstrates that this is not true. While the majority of the 15 tips tested on oxidized Ag yield a non-linear I-V curve (curve 2 in Fig. 3a), a few tips yield a linear current response. Similar behavior was found during the I-V measurements on HOPG using Pt-Ir tips (Fig. 3b); both linear and non-linear I-V curves were observed, dependent only on the tip. However, we note, that tip crashes on the oxidized Ag surface are frequently observed when the set point resistance is programmed to lower values ($< \sim 100$ MΩ), whereas on gold or HOPG, set point resistances as low as 1 MΩ can be routinely used with Pt-Ir tips. This difference is most likely due to the oxide layer on the Ag surface, which constitutes an (additional) barrier for the tunneling electrons. Apparently, the degree of non-linearity in the I-V response depends only on the structure of the tip.

In consideration of the above arguments and experimental findings we formulate the following hypothesis to explain the non-linear I-V response on Au, Ag and HOPG surfraces: *While ramping the bias voltage in the TS experiment, the tip experiences an electric field induced mechanical stress. Above a tip-specific threshold, this stress can result in tip-elongations (contractions) upon increasing (decreasing) the electric field between tip and sample. In such a case, the geometrical tunneling barrier width s increases (decreases) upon decreasing (increasing) the bias voltages. The tip-sample distance s is not constant and the tunneling current becomes a non-linear function of the bias voltage.*

Conclusive evidence for this hypothesis is obtained from the following experiments: I-V measurements with Au tips on the reconstructed Au(111) surface (Fig. 4) yield a *linear* I-V response only when the bias voltage scan window is small ($-0.5\ V \leq V_b \leq +0.5V$). Both tip and surface remain stable during these low voltage I-V scans as is evidenced by the image shown in Fig. 4b, which was taken immediately after the I-V measurement over the same area. Upon increasing the bias voltage scan window (0 to -3V)

in a second I-V measurement using the same tip on exactly the same surface location, a strongly non-linear I-V curve is recorded (Fig. 4c). In the bias voltage range between 0 and -0.5 V the current rises linearly. At voltages more negative than -0.5V the current increases nearly exponentially until it abruptly drops to virtually zero at ~-2V. Imaging the surface after this TS experiment (Fig. 4d) shows the presence of the end of the tip in the area where the TS experiment was performed (Fig. 4c). On the basis of our hypothesis, the interpretation of the result shown in Fig. 4 is straightforward. The mechanical stresses exerted by the electric field between tip and sample elongate the tip at bias voltages more negative than -0.5 V. At bias voltages around -2V, the field induced stress increases until the tip specific maximum stress is reached and the tip fractures, causing the abrupt current drop in Fig. 4c. Local heating of the tip apex region, as suggested by Tsong[27], might enhance the field stress induced plastic response of the tip at high biases and currents. Further enhancement may occur in clean (metallic) tip - (metallic) sample tunnel junctions, when the tip - sample gap spacing becomes small enough to allow for strong adhesive forces[28,29]. Thus, adhesion forces are likely to occur in a gold tip-gold sample junction, even in air, because of the relative chemical inertness of gold. However, adhesion forces are expected to be smaller for oxidized tip-sample systems (e.g. Pt-Ir/Au(111) and Pt-Ir/oxidized Ag). Tip fracture was observed in the range from |2V| and up for Au/HOPG, Pt-Ir/Au and Pt-Ir/Ag systems..

Mamin et. al.[13] reported mound formations on an Au(111) surface in STM experiments using an Au tip upon applying voltage pulses of 3 to 5V pulse height. These researchers suspected that a field evaporation mechanism causes gold deposition form the tip on the surface. Field stress induced tip fracture was excluded in Mamin et. al.'s study because the voltage pulse duration was on the order of some 100 nsec, which makes a plastic response of the tip seem unlikely. In our case, however, the bias voltage is ramped sufficiently slow (~0.5 sec) to allow for plastic deformation and, in some cases, fracture. .Assuming a parallel plate geometry and a tip-sample distance of 5Å, we estimate the local

electric field E at a bias voltage of 2V in our STM experiment to ~0.4 V/Å, which results in a combined normal and shear stress at the tip apex $\sigma = 0.5\varepsilon_0 E^2 \approx 7 \times 10^9$ N/m$^2$ ($\varepsilon_0$ : vacuum dielectric constant). This estimate demonstrates that the stresses encountered in our experiments are at least of the order of the maximum tensile stress of polycrystalline gold (~1. X $10^8$ N/m$^2$). Therefore, plastic tip deformations might be expected even for polycrystalline tip materials with higher elastic moduli and correspondingly higher tensile strength, e.g., Pt, Ir and W. A largely defect free, crystalline tip apex, however, should be stable even at much higher field strength[14].

Electric field induced mechanical stresses that induce non-linear features in the I-V curve should also be absent, when the tip is *replaced* by a *crystalline, flat surface* in the TS experiment. We realized an approximation for such an arrangement by replacing the sharp STM tip with a second spherical Au ball and by measuring the tunneling current between (111) facettes of the two Au-spheres. The "image" generated by two smooth surfaces scanning across each other is featureless. Tip-like hillocks on either one of the surfaces are easily detected in this arrangement, when the STM is used in the image mode. The presence of tip-like clusters or hillocks on one of the surfaces yields significant height variations upon scanning, sometimes even with appreciable spacial resolution as shown in Fig. 5a. The current voltage characteristic of the two specimens used to obtain the image in Fig. 5a shows the characteristic non-linear features within the scan voltage window of -1.5V < $V_b$ < 1.5V, which are indicative of field induced tip elongation. The I-V characteristic of specimen yielding a featureless image, however, is *always* linear within the scan voltage window of 4V and for a wide range of initial tunnel gap spacings (Fig. 5c).

In the following section, we describe a few more examples of combined current voltage and STM measurements, which demonstrate the variety of field stress induced phenomena. All these experiments were performed with Pt-Ir tips on reconstructed Au(111) surfaces. The I-V measurement performed after having taken the initial image in

Fig. 6a yields a strongly non-linear I-V curve (Fig.6b). An image of this area taken after the I-V measurement shows that a hole has been formed on the surface where the tip was located during the I-V measurement (Fig. 6c). Again, these findings can be explained on the basis of our hypothesis. At the beginning of the voltage ramp (+2V in Fig. 6b) the tip elongates, giving rise to a current increase even for decreasing bias voltages. The current then abruptly reaches a region in which it decreases noisily, but overall linear as a function of bias voltage. Below ~0.6V a strongly non-linear decrease is observed and finally a linear decay sets in at ~0.5V. Fig. 6d shows the results of a separate I-V measurement performed with the same tip, but on a different part of the Au-surface. This experiment also resulted in the creation of a hole in the surface, similar to the one shown in Fig. 5c. The larger bias voltage scan in Fig. 6d yields a current behavior similar to the one shown in Fig. 6b (i.e., the current increase for decreasing bias voltages at the beginning of the scan at +2.5 V, an abrupt transition to a region of slower linear decay is observed between 2.3 and 1.7 V, followed by a strong nonlinear I-V response, and finally a linear I-V behavior for voltages less that 0.5V ).

We suspect, that the holes created during the current-voltage measurements are due to a mechanical contact between tip and sample, rather than to a field emission or evaporation process. Closer inspection of the images in Fig. 6a and 6c reveals, that the reconstruction features are deformed in the area below the hole in Fig. 5c, which is to be expected as a consequence of mechanical stress, supporting our suspicion. Field induced lifting of reconstruction features, which is usually observed at higher positive sample biases, should be weakened in case of tip sample contact because of a local breakdown of the field expected in such a case. We assume that the tip is in contact with the surface in the bias voltage range between the current peaks in the high voltage regimes (1.9V in Fig. 5b and 2.8V in Fig. 5d) and the onset of the strongly non-linear decrease below 0.6 V in Fig. 5b and 1.9 in Fig. 5d (see arrows). A strongly non-linear current decrease is expected to occur, when the tip contracts and lifts off the surface upon lowering the bias voltage. As

mentioned above, heat generation and dissipation in the tip apex region might enhance the field induced plastic tip deformation. Since no additional material was detected on the surface after these I-V measurements, we assume an elastic tip response to the field stress. In that case the critical fields at which tip-sample contact occurs should increase with the initial tip-sample distance (the latter is determined by the initial set point resistance, see experimental section), since, from Hooke's law ($\Delta s_e = c_t \sigma$ where $c_t$ is the tip "spring constant") the tip elongation, $\Delta s_e$, is proportional to the field induced stress, $\sigma$. For the same reason, the voltage interval of closed contact should decrease with increasing initial tip sample distance. On the basis of our definition of the contact range, this trend is clearly seen by comparing Fig. 5b with Fig. 5d. (note the set point values in the figure captions). The average value of the resistance during contact amounts to ~130 MΩ in both curves shown in Fig. 5. Experimental work of Gimzewski and Möller[30] and calculations of Lang[31], however, show that the resistance for a *clean* metallic tip-sample point contact is of order $h/2e^2$ (~10kΩ) for contact apertures of atomic dimensions (i.e., the "constriction" or "Sharvin" resistance, see also [32-35]). As is evidenced by the hole in the surface (Fig. 5c), the contact aperture *a* during the I-V measurement in Fig. 5b was about 20Å. This is clearly in the range of a constriction aperture, even at room temperature, since the electron mean free path *l* is ~$10^{-6}$ cm, and the requisite condition for a constriction ($l/a >> 1$) is satisfied. In order to explain the high value of the contact resistance measured here, we have to assume that the tip was contaminated (e.g., oxidized) in our experiment. Further evidence for this assumption comes from the fact that the tip-sample contact resulted consistently in the formation of a hole rather than a protrusion in the surface, which indicates weak adhesion between tip and sample[30]. Thus, in our experiment the electrons cannot travel freely (ballistically) from one metal into the other, but still have to tunnel through a barrier, even during mechanical contact conditions. Inspection of Fig. 5d reveals a small region of high current between the contact closing point (current peak at ~2.4V) and the onset of the slow linear current decrease at ~2.2V. In the realm of the aforementioned

contamination barrier $\phi_c$ we tentatively attribute this region of high current to ballistic electron transport *over* $\phi_c$. The region of linear current decrease below 2.1V then corresponds to regular tunneling *through* $\phi_c$. Consequently, from Fig. 5d we estimate the energetic height of $\phi_c$ to ~2.2eV. This speculation is consistent with the I-V curve shown in Fig. 5b (obtained with the same tip), where only an approximately linear current decrease in the bias voltage interval of closed contact (0.6 to 1.9V) is observed, since the applied potential is too low to allow for ballistic transport over $\phi_c$. However, the basic physics underlying our proposed mechanism of electric field induced tip elongations, supported by a number of experimental findings, should be unaffected by this contamination layer.

In the last example (Fig.7), we show that atomic emission from the tip can also be observed in combined TS-STM experiments: ramping the bias voltage during one I-V measurement (Fig. 7b) decorates the initially clean reconstructed Au (111) surface shown in Fig 6a with particles of atomic dimensions (Fig. 7c). Therefore, we assume that the "noise"-pattern observed in the I-V curve above bias voltages of ~0.5V (Fig. 7b) is related to the emission of single atoms or small clusters from the tip. The fact that the current remains measurable and even increases during the I-V measurement (Fig. 7b) suggests that the particles are not emitted from the tip apex but from regions along the tip shank. This suggestion also explains why the particles are not concentrated in the region of the tip location during the I-V measurement (in the center of the images shown in Fig. 7), but are spacially distributed over a relatively large area. Since the particles order on the reconstructed Au(111) surface in a pattern which is very similar to the adsorption pattern previously reported for sub-monolayer coverages of Ni on reconstructed Au(111)[36], we assume, that the particles are metallic.

Finally, we would like to point out that the electric field induced tip elongation clearly also affects the measured value of the apparent barrier height $\phi_{eff}$. To demonstrate this, we measured the current decay as a function of tip-sample distance (I vs. s) for

different initial set point - bias voltages in a (Au tip) / ($\sqrt{3}$ x 22 Au(111) sample) tunnel junction (Fig. 8). The I-V curve of this system, measured in the bias voltage range -1V$\leq$ $V_b \leq$+1V, is characteristic for an elastic, field induced tip elongation since the current response is strongly non-linear in the high field range ($V_b$ > |0.5|) and linear in the low field regime, for low initial set point bias voltages (+0.2 V for curve 1 in Fig. 7a). For higher initial set point bias voltages (+0.8 V for curve 2 in Fig. 8a), the non-linearity becomes even more pronounced since the tip is already in an elongated state when bias voltage ramping begins (switching between the initial set point bias and the bias at which the voltage ramp begins in the I-V measurement occurs within a time less than a millisecond, which is apparently too short to allow for a significant tip contraction). Since the tip contracts from the initial elongated state upon lowering the bias, higher initial set point biases result in a more pronounced non-linearity in the I-V curve. In this way, I-V curves can be generated which appear to reflect a current blockade for lower bias voltages during the I-V measurement, simply because the tip apex is too far away from the surface in the low voltage regime. However, as long as the field induced stresses are kept within the elastic limit of a particular tip, one can switch back and forth between the curve shapes shown in Fig. 8a by changing the initial set point bias. Consequently, a completely linear I-V curve is obtained when both the initial set point bias voltage and the voltage scan window are sufficiently small (cf. Fig. 3a). Therefore, it should be easy to distinguish between a real coulomb blockade[8,9] and an artificial tip elongation/contraction effect. Tip elongation at higher initial set point biases is reflected also in the I vs. s measurements (Fig.8b). When the initial set point bias voltage is set in the range where a linear I-V curve is obtained (Fig. 8a, curve 1), the current decays rapidly as a function of s (Fig. 8b, curve 1) and a physically reasonable value of ~3.5 eV is obtained for the apparent barrier height. When, on the other hand, the initial set point bias voltage is fixed in the range of elastic tip deformations (0.8V in Figs. 8a and 8b, curve 2) the current decays slowly as a function of s, yielding an extremely low barrier height of ~0.1eV. Image potential effects, which are

known to affect the apparent barrier height[34] cannot account for this dramatic change as a function of bias voltage. The suggested deformation mechanism, however, provides a simple explanation. The tip-sample distance might be very small under deformed tip conditions, yielding a low apparent barrier height[37], and, since the tip is deforming, the actual tip displacement does not coincide with the nominal tip displacement determined by the z-piezo voltage (this is the scale used for the abcissae in Fig. 8b). The same phenomenon is observed in barrier height measurements on Au(111) using Pt-Ir tips. Low barrier heights are obtained from I-$\Delta$s measurements when the I-V curve is non-linear, indicating tip elongation. Conversely, reasonable values of $\phi_{eff}$ (2-4 eV) are obtained when the I-V curve is linear. Since we have to assume that all tips operated in air are contaminated (oxidized), with the possible exception of Au-tips, this, of course, also means that physicially reasonable effective barrier heights are expected even for tips which are most likely to be contaminated. Provided that the contamination layer is geometrically thin enough, this finding is not too surprising considering that adsorbates most likely encountered in ambient air yield work function changes of $\sim\pm$1eV on metals (neglecting alkali adsorbates).

### *Conclusions*

Our experiments demonstrate that the electric field in an STM can alter both the tip and the sample surface structure. In particular, we have shown that the electric field between tip and sample can induce transitions between the $\sqrt{3}$ x 22 and the 1x1 phases of the Au(111) surface during I-V measurements. Therefore, meaningful I-V measurements (and especially (dI/dV) measurements) should always be checked by imaging the probed surface areas. At this stage, we cannot critically compare our results to the recent findings of Kaiser et. al.[5] and Everson et. al.[6,7] who detected a surface state at $\sim$+0.5eV on the reconstructed Au(111) surface in TS experiments using tungsten tips, since these researchers used a modulation technique to directly measure the (dI/dV) vs. V spectrum.

This greatly enhances the dynamic range of the current measurement as compared to our experiments.

*Stable* Pt-Ir tips yield a *linear* current-voltage response on Au(111), graphite and oxidized Ag surfaces in the tested bias voltage range $-3V \leq V_b \leq +3V$, which indicates that the tunneling electron always finds an empty final state with constant probability.

Structurally *unstable* Pt-Ir tips and all tested Au tips yield a linear I-V response in a small voltage range around 0V, when the initial sample bias voltage is below ~|0.5V|. For bias voltages $V_b > \sim|0.5V|$, these tips yield strongly non-linear I-V curves, which can be explained on the basis of electric field induced tip deformations. Elastic tip deformations caused by adhesion forces were suspected by Wintterlin et. al[38] and Doyen et. al.[39] to explain the atomically resolved STM topographs of Al(111). Aluminum is considered to be an ideal nearly free electron metal, which therefore should not exhibit atomic corrugation in STM images if the Tersoff-Haman theory[40] fully describes the physical principles of STM imaging. Thus, both adhesion and, as shown in this paper, electrostatic forces play an important role in STM. Since we have shown that elongated tips yield a low value for the apparent barrier height, we might suspect, that the extremely low apparent barrier heights frequently reported in electrochemical STM studies[41], where the tip is immersed in an electrolyte, are also, at least partly, related to plastic tip deformation effects (other possible mechanisims are suggested by Sass and Gimzewski[42]). Picturing the tip as a "model ion", we might assume, that a solvation shell of solvent molecules forms around the tip apex. As in the dissolution process of salts in solvents, this solvation shell might lower the interatomic bond energy in the tip apex region. Consequently, a solvated tip apex should be more susceptible to plastic deformations, caused either by electrostatic or adhesive forces between tip and sample. Since most theoretical and experimental work concerning force-mediated tip-sample interactions was focussed on adhesion forces[27,28,34,43] we feel that electric field related aspects of tunneling deserve more attention in future STM work.

**Acknowledgements**

This work was funded by the Office of Naval Research. One of us, JHS, would like to thank the Deutsche Forschungsgemeinschaft for support under grant no. Sch 428 / 1-1.

## Figure Captions

Fig.1 STM images and current-voltage curves obtained in sequential order on a $\sqrt{3}$ x 22 reconstructed Au(111) surface. (a): initial image of the reconstructed surface; (b): current-voltage curve for negative bias voltage excursions; (c): image of the surface after the I-V measurement shown in (b); (d): current-voltage curve for positive bias voltage excursions; (e): image of the surface after the I-V measurement shown in (d); the reconstruction is partially lifted (see text). $I_{set}$ =1 nA, $V_{set}$=-0.15 V for all images and I-V curves.

Fig. 2 STM images and current-voltage curves obtained in sequential order on a $\sqrt{3}$ x 22 reconstructed Au(111) surface. (a): initial image with an unreconstructed section in the center generated as shown in Fig. 1d and 1e; (b): current-voltage curve for negative bias voltage excursions; (c): image of the surface after the I-V measurement shown in (b); new reconstruction features are forming; (d) current-voltage curve for more negative bias voltage excursions; (e): image of the surface after the I-V measurement shown in (d) showing more new reconstruction features which seem to center around the tip location during the I-V measurement; (f): current-voltage curve for bipolar bias voltage excursions; (g): image of the surface after the I-V measurement shown in (f); (h): current-voltage curve for higher bipolar voltage excursions; (i): image of the surface after the I-V measurement shown in (h). (see text). $I_{set}$= 1nA, $V_{set}$=-0.15 V for all images and I-V curves.

Fig. 3 Current-voltage curves obtained with Pt-Ir tips on oxidized Ag and HOPG surfaces. (a): oxidized Ag-surface; $I_{set}$=0.6 nA, $V_{set}$=+1 V (curve 1); $I_{set}$=0.5 nA, $V_{set}$=0.7 V (curve 2); (b): HOPG-surface; $I_{set}$=1.5 nA, $V_{set}$=0.1 V for both curves. (see text).

Fig. 4 Current-voltage curves and STM-images obtained with an Au-tip on a $\sqrt{3}$ x 22 reconstructed Au(111) surface. (a): current-voltage curve for small bipolar bias voltage excursions; $I_{set}$=3 nA, $V_{set}$=-0.09 V; (b): image of the surface obtained after the I-V measurement shown in (a); (c): current-voltage curve for a high negative bias voltage excursion; $I_{set}$=0.5 nA; $V_{set}$=-0.3 V; (d): image of the surface obtained after the I-V measurement shown in (c). $I_{set}$=5 nA and $V_{set}$=0.15 V for all images.

Fig. 5 Current-voltage curves and STM-images obtained by replacing the tip with a second facetted Au-sphere. (a): STM-image showing reconstruction features on one of the surfaces; the resolution results from a tip-like cluster or hillock on one of the Au spheres; (b): current-voltage curve obtained with the spheres used in the imaging experiment shown in (a); (c): Current-voltage curves me sured between two smooth facetted spheres yielding a featureless image. (1) $I_{set}$=0.8 nA, $V_{set}$=-2.0V; (2) $I_{set}$=0.8 nA,$V_{set}$=0.75 V; (3) $I_{set}$=0.8 nA, $V_{set}$=-0.25 V; (4) $I_{set}$=0.8 nA, $V_{set}$=-0.125 V.

Fig. 6 Current-voltage curves and STM-images obtained with a Pt-Ir tip on a $\sqrt{3}$ x 22 reconstructed Au(111) surface. (a): initial image of the reconstructed surface; (b) I-V curve for positive bias voltage excursions; $I_{set}$= 1.46 nA, $V_{set}$=0.2 V; (c) image of the surface obtained after the I-V measurement shown in (b) $I_{set}$=2.5 nA, $V_{set}$=0.2 V; (d): I-V curve for more positive bias voltage excursions; $I_{set}$=1 nA, $V_{set}$=1.25 V. (see text).

Fig. 7 Current-voltage curves and STM images obtained with a Pt-Ir-tip on a $\sqrt{3}$ x 22 reconstructed Au(111) surface. (a): initial image; $I_{set}$=4.5 nA, $V_{set}$=-0.17 V. (b): I-V measurement for negative bias voltage excursions; $I_{set}$=1 nA, $V_{set}$=-0.2 V. (c): image of

the surface obtained after the I-V measurement shown in (b). The surface is decorated with particles of atomic dimensions (see blow-up in the insert). $I_{set}$=4.5 nA, $V_{set}$=-0.17 V.

Fig. 8 I-V and I vs. Δs measurements obtained with an Au tip over a fixed location on a reconstructed Au(111) surface. (a) I-V curves measured for two different set point resistances. curve (1): $I_{set}$=1 nA., $V_{set}$= 0.15 V; curve (2): $I_{set}$=1 nA, $V_{set}$=0.75 V. (b) I vs.Δs curves obtained with the same set point values as in (a). (see text).

References


1. G. Binnig, K.H. Frank, H. Fuchs, N. Gracia, B. Reihl, H. Rohrer, F. Salvan and A. R. Williams, Phys. Rev. Lett., **55(9)**, 991 (1985)
2. R. M. Feenstra and P. Martesson, Phys. Rev. Lett., **61(4)**, 447 (1988)
3. P. N. First, I. A. Stroscio, R. A. Dragoset, D. T. Pierce, and R. J. Celotta, Phys. Rev. Lett., **63(13)**, 1416 (1989)
4. Y. Kuk and P. J. Silverman, J. Vac. Sci. Technol. A, **8(1)**, 289 (1990)
5. W. J. Kaiser and R. C. Jaclevic, JBM J. Res. Develop., **30 (4)**, 411 (1986)
6. M. P. Everson, R. C. Jaclevic and W. Shen, J. Vac. Sci. Technol. A, **8(5)**, 3662 (1990)
7. M. P. Everson, L. C. Davis, R. C. Jaclevic and W. Shen, J. Vac. Sci. Technol. B, **9(2)**, 891 (1991)
8. P. J. M. van Bentum, H. van Kempen, L. E. C. van der Leemput and P. A. A. Teunissen, Phys. Rev. Lett., **60(4)**, 801 (1989)
9. R. Wilkins, E. Ben-Jacob and R. C. Jaclevic, Phys. Rev. Lett., **63(7)**, 801 (1989)
10. J. Hossick Schott and H. S. White, Langmuir, in press
11. For a recent review see: "J. A. Stroscio and D. M Eigler, Science, **254,** 1319 (1991)", and references therein.
12. L. J. Whitman, J. A. Stroscio, R. A. Dragoset and R. J. Celotta, Science, **251**, 1206 (1991)
13. H. J. Mamin, P. H. Guethner and D. Rugar, Phys. Rev. Lett., **65(19)**, 2418 (1990)
14. R. Wagner, *Field Ion Microscopy in Materials Science* (Springer-Verlag, Berlin, Heidelberg, New York, 1985)
15. P. J. Birdseye and D. A. Smith, Surf. Sci., **23**, 198 (1970)

16. A. Kiejna, Sol. Stat. Commun., **50(4)**, 349 (1984)

17. Digital Instruments, Nanoscope II Manual

18. J.G. Simmons, J. Appl. Phys., **34**, 1793 (1963)

19. Hsu T., Cowley, J. M. Ultramicroscopy , **11**, 125 (1983)

20. Ch. Wöll, S. Chiang, R. J. Wilson and P.H. Lippel, Phys. Rev. B, **39(11)**, 7988, (1989)

21. J. V. Barth, H. Brune, G. Ertl and R. J. Behm, Phys. Rev. B, **42(15)**, 9307, (1990)

22. W. Haiss, D. Lackey, J. K. Sass and K. H. Besocke, J. Chem. Phys., **95(3)**, 2193 (1991)

23. J. Jahanmir, P. E. West and T. N. Rhodin, Appl. Phys. Lett, 52(4), 2086 (1988)

24. M. A. Ramos, S. Viera, A. Buendia and A. M. Baro, J. of Microscopy, **152(1)**, 137 (1988)

25. A. Brodde, St. Tosch and H. Neddermeyer, J. of Microscopy, **152(2)**, 441 (1988) .

26. J. H. Coombs and J. B. Pethica, IBM J. Rev. Develop., **30(5)**, 455 (1986)

27. T. T. Tsong, as referenced in 11

28. U. Dürig, O. Züger and D. W. Pohl, Phys. Rev. Lett., **65(3)**, 349 (1990)

29. J. B. Pethica and W. C. Oliver, Phys. Scr., **19A**, 61 (1984)

30. J. K. Gimzewski and R. Möller, Phys. Rev. B, **36(2)**, 1284 (1987)

31. N. D. Lang, Phys. Rev. B, **36(15)**, 8173, (1987)

32. Y. V. Sharvin, Sov. Phys. JETP, **21**, 655

33. A. G. M. Hansen, A. P. van Gelder and P. Wyder, J. Phys. C., **13**, 6073 (1980)

34. R. Landauer, Z. Phys. B, **68**, 217, (1987)

35. S. Ciraci and E. Tekman, Phys. Rev. B, **40(17)**, 11969 (1989)

36. D.D. Chambliss, R. T. Wilson and S. Chiang, J. Vac. Sci. Tech. B, **9**, 2933 (1991)

37. N. D. Lang, Phys. Rev. B, **37(17)**, 10395 (1988)

38. J. Wintterlin, J. Wiechers, H. Brune, T. Gritsch, H. Höfer and R. J. Behm, Phys. Rev. Lett., **62**( ), 59 (1989)

39. G. Doyen, E. Koetter, J. Barth and D. Drakova, in *Scanning Tunneling Microscopy and Related Methods*, edited by R. J. Behm, N. Garcia and H. Roher, Nato Asi Series E 184

40. J. Tersoff and D. R. Haman, Phys. Rev. B, **31(2)**, 805 (1985)

41. M. Binggeli, D. Carnal, R. Nyffenegger, H. Siegenthaler, R. Christoph and H. Rohrer, J. Vac. Sci. Technol. B, **9(4)**, 1985 (1991)

42. J. K. Gimzewiski and J. K. Sass, in *Proc. ICTP Conf. on Cond. Matter Physics Aspects of Electrochemistry* , Trieste, Italy, (1990), edited by. M. P. Tosi and A. A. Kornyshev (World Scientific, Singapure, New Yersey, 1991)

43. S. Ciraci, and A. Baratoff, Phys. Rev. B, **41(5)**, 2763 (1990)

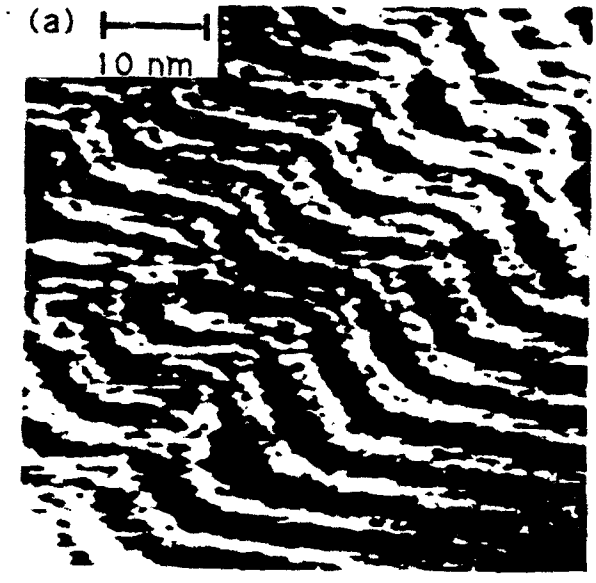


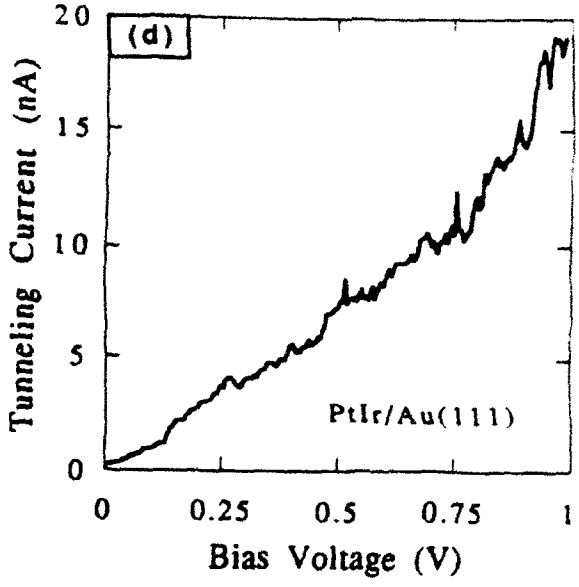


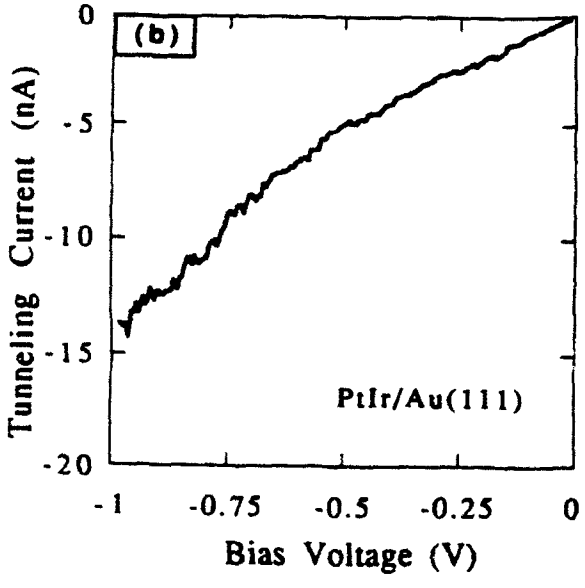


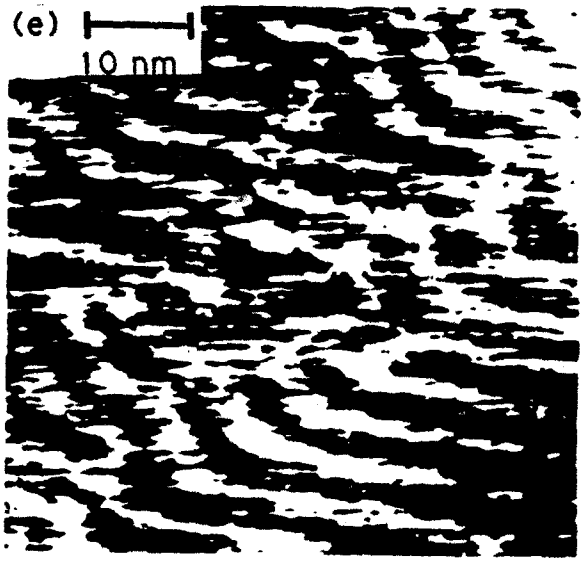


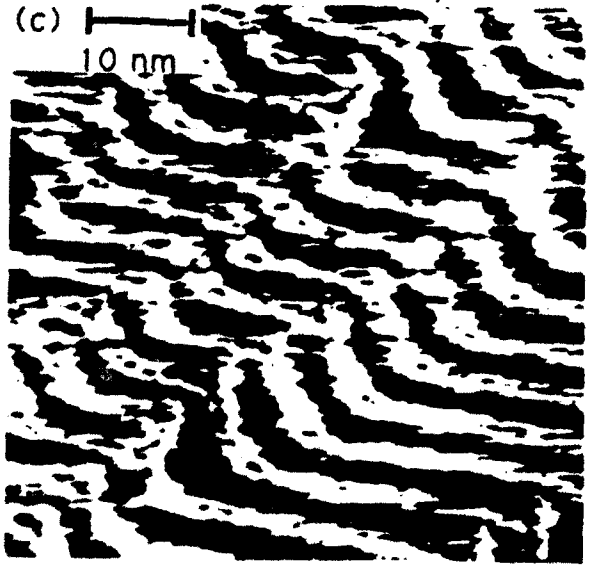


**Hossick Schott, White Fig. 1**

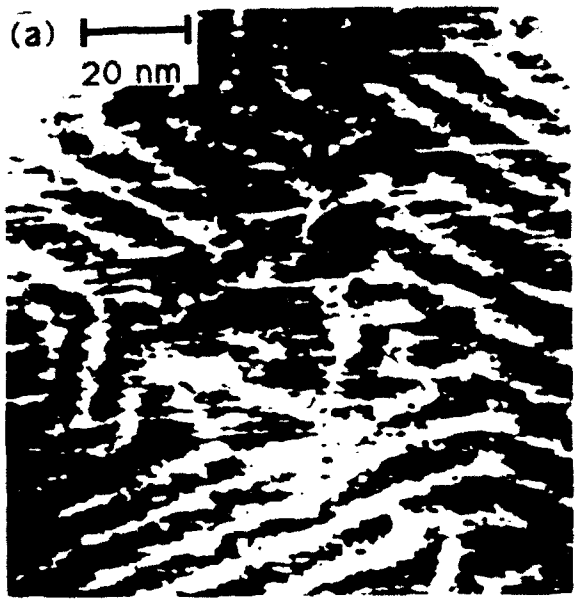


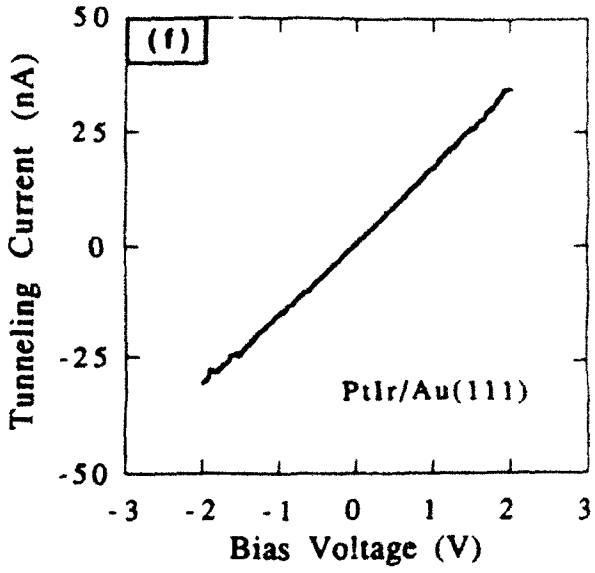


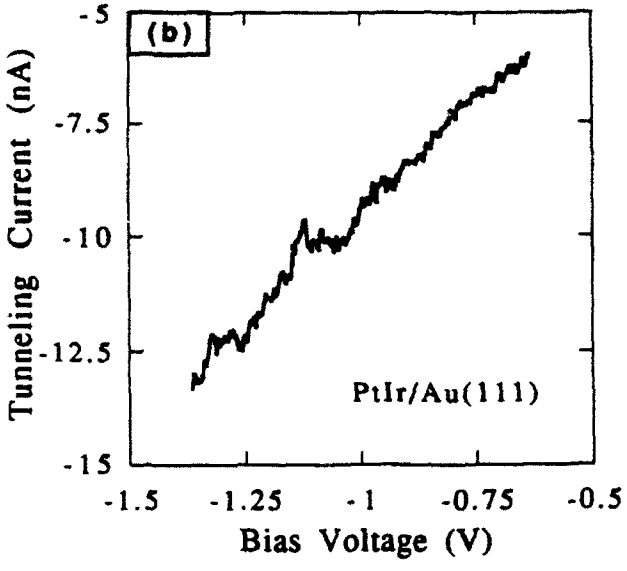


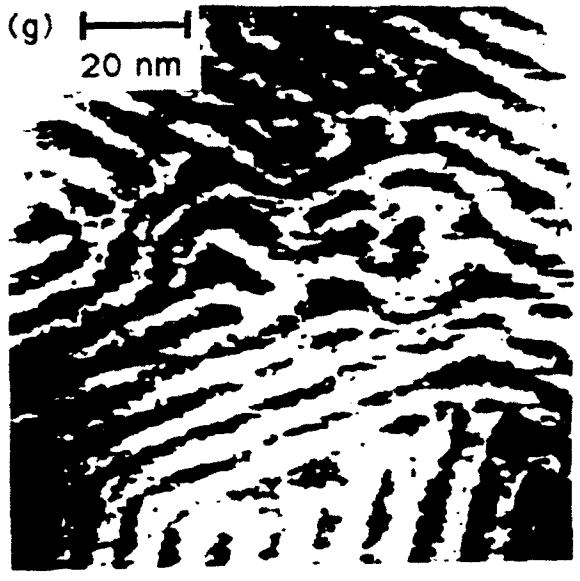


**Hossick Schott, White Fig 2, part 1**

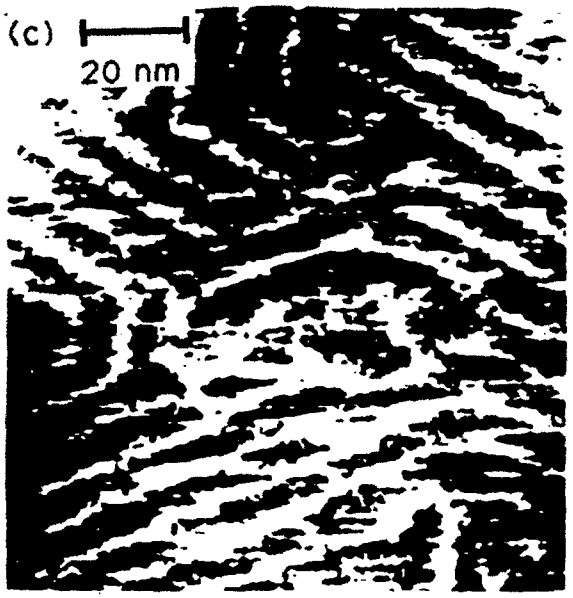


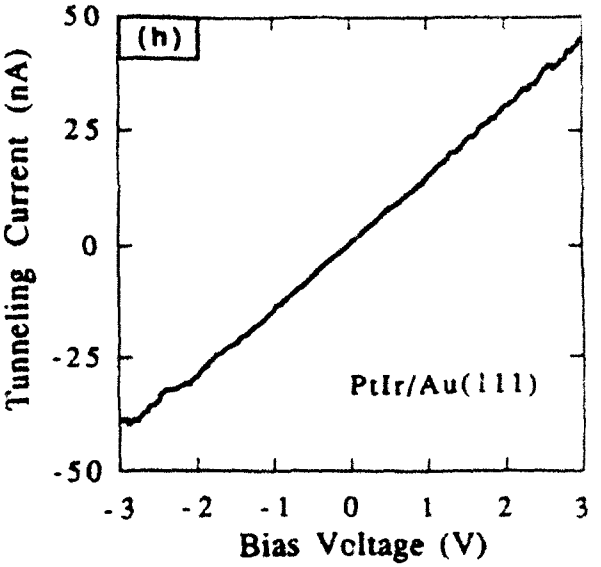


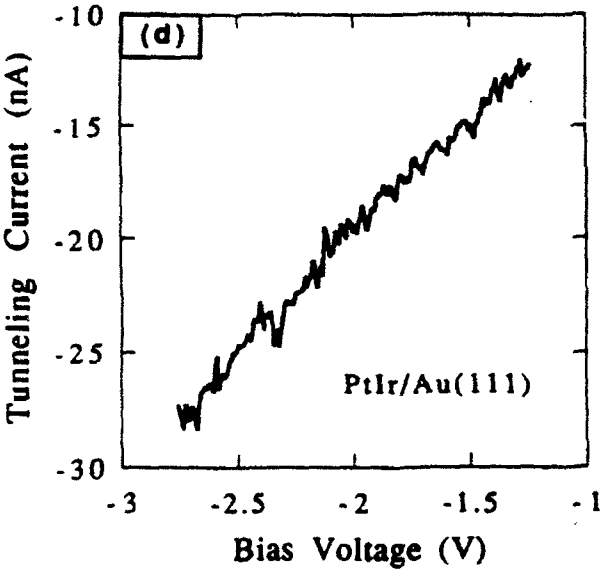


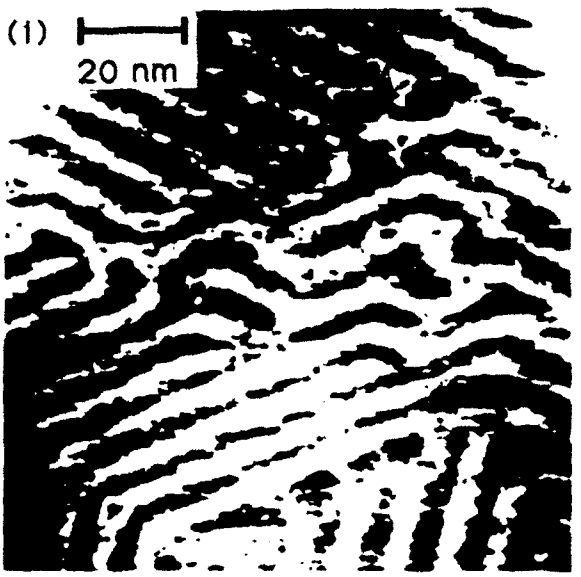


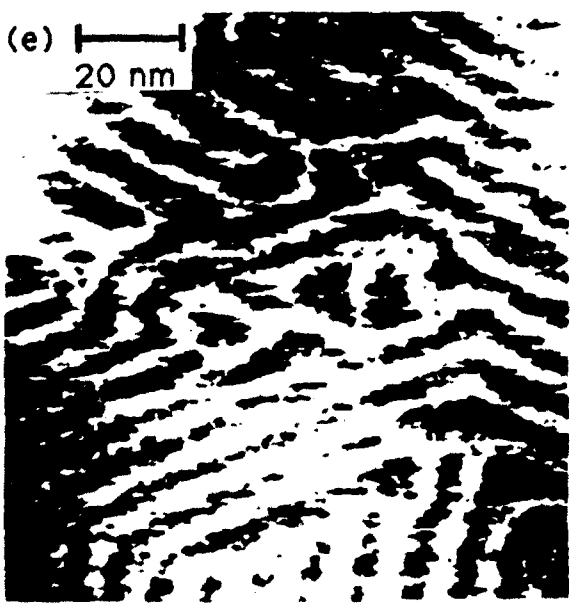


**Hossick Schott, White Fig 2, part 2**

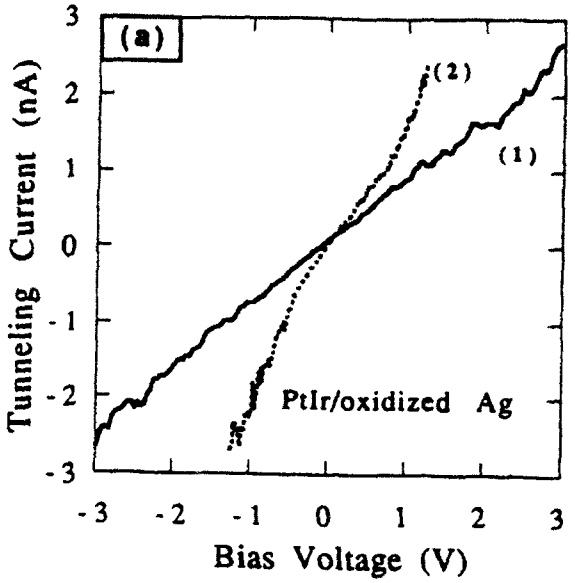


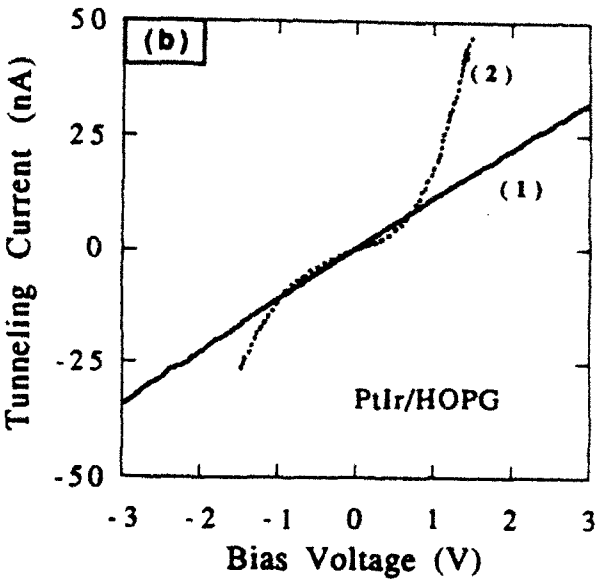


**Hossick Schott, White Fig. 3**

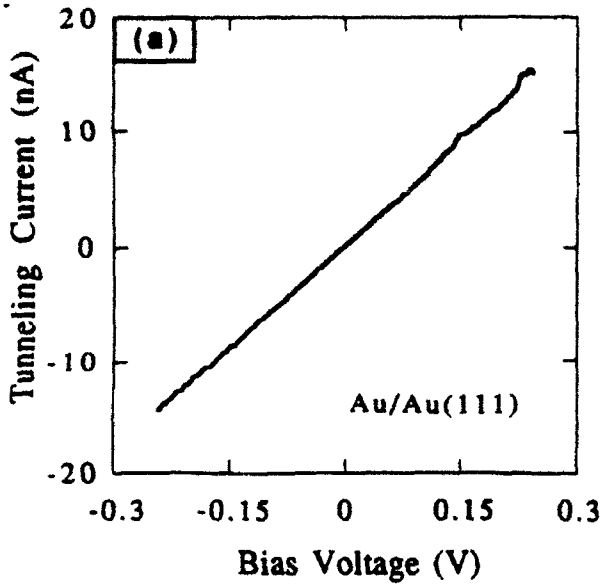


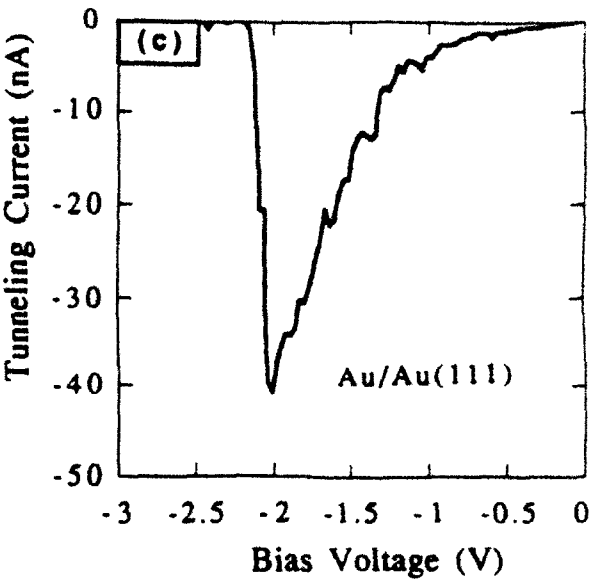


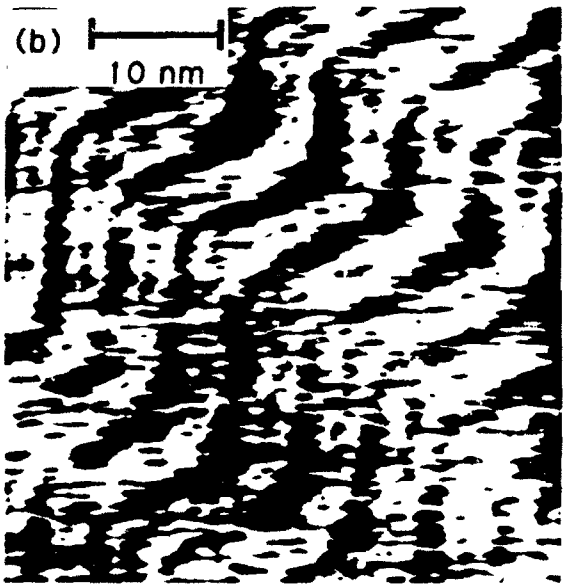


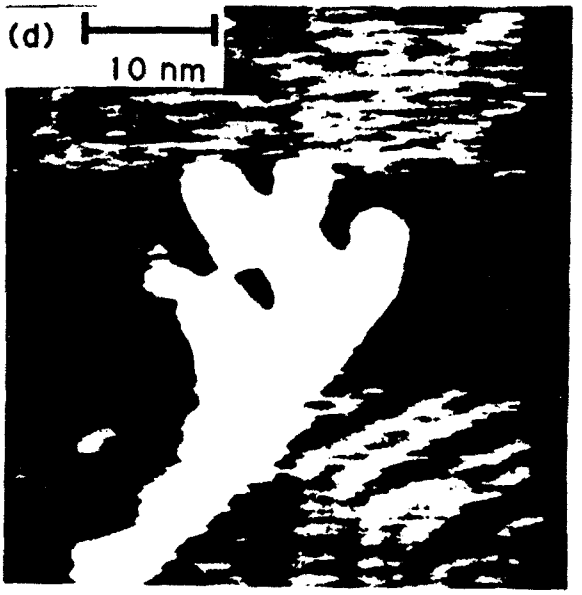


**Hossick Schott, White Fig 4**

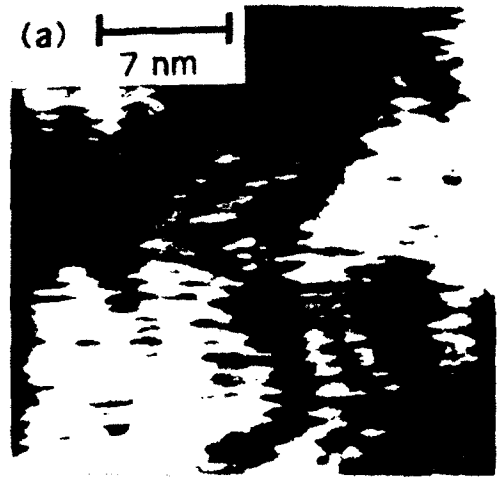


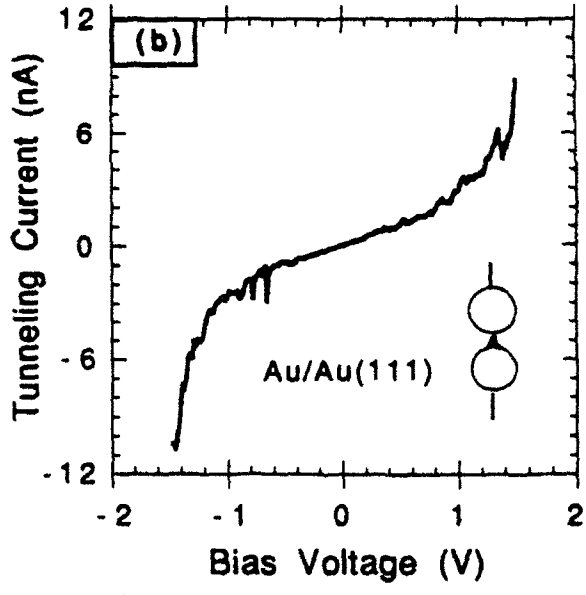


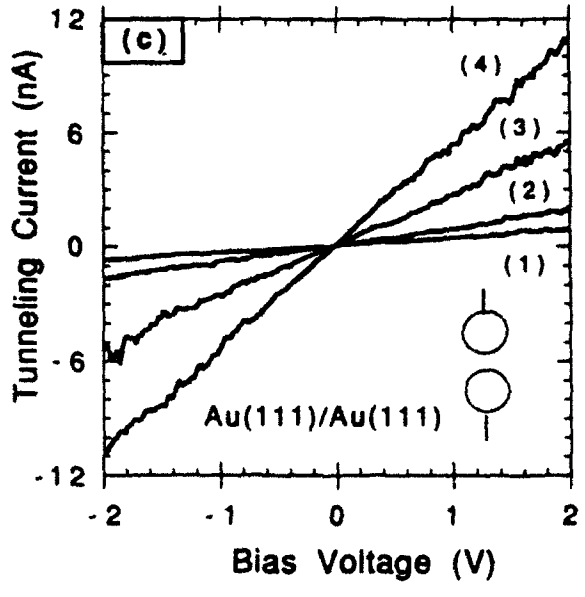


**Hossick Schott, White Fig 5**

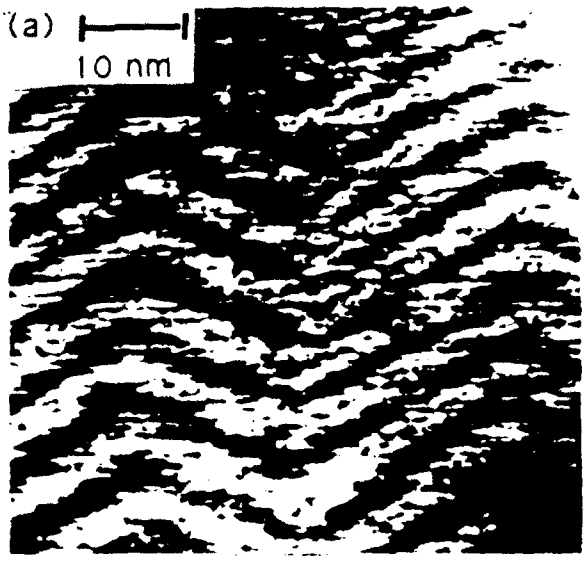


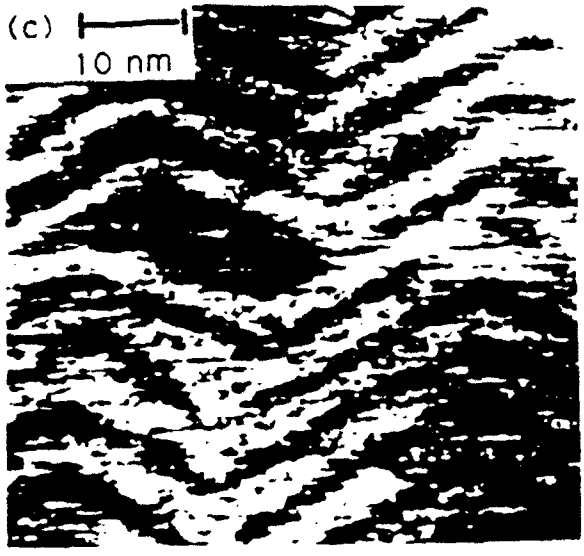


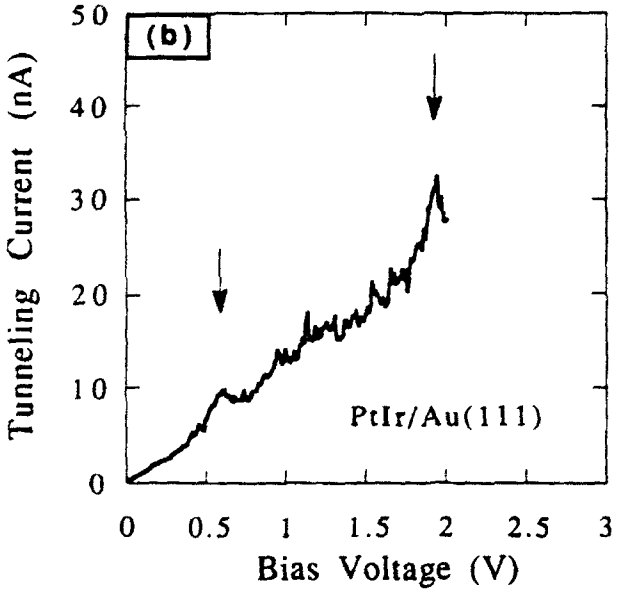


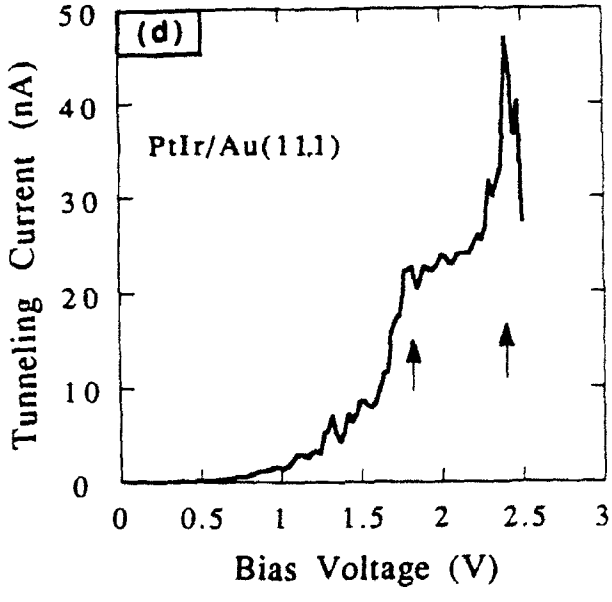


**Hossick Schott, White Fig. 6**

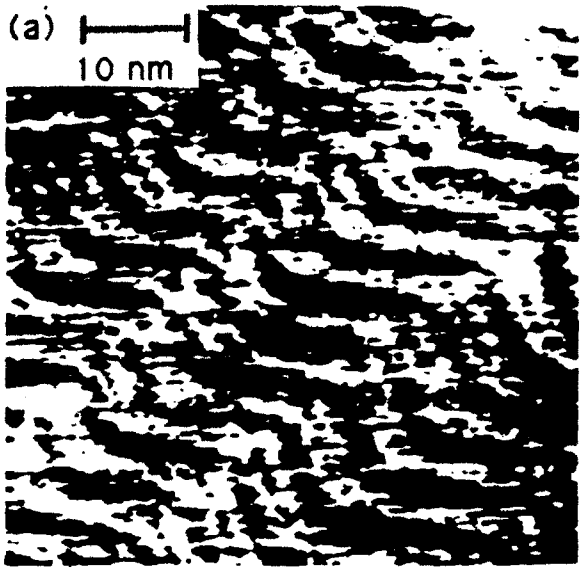


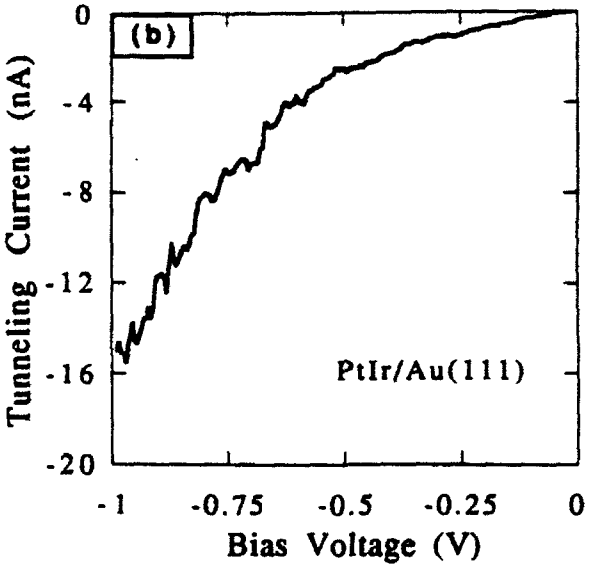


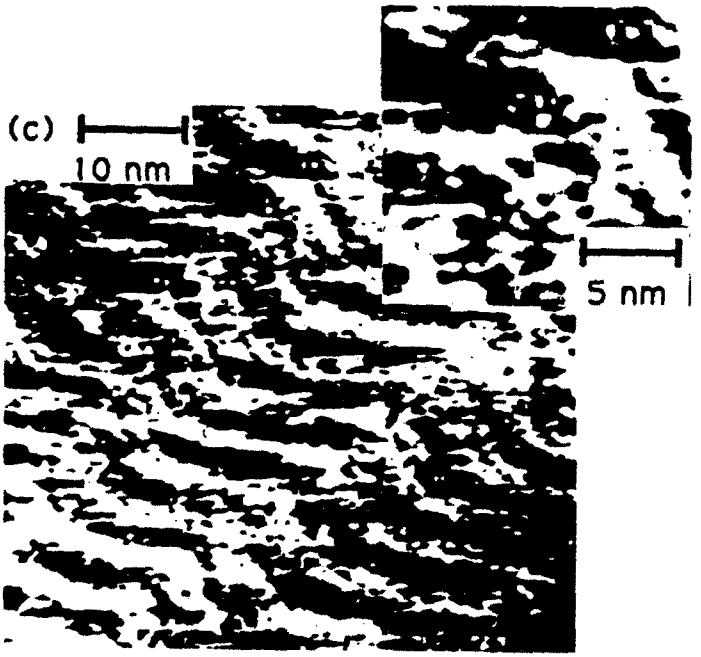


Hossick Schott, White Fig. 7

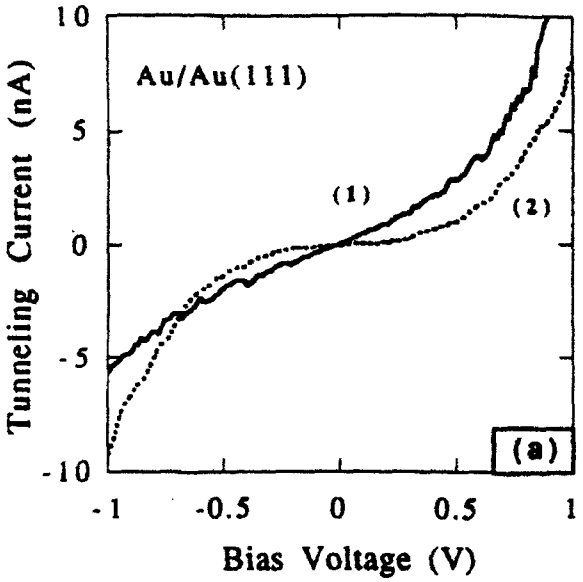


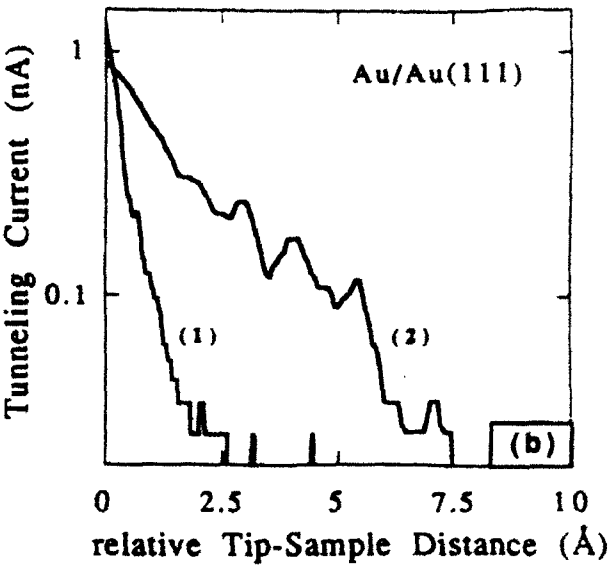


**Hossick Schott, White Fig. 8**